

# CREEP RUPTURE OF SPECIMENS WITH RANDOM MATERIAL PROPERTIES

HANS BROBERG

The National Institute for Material Testing, Borås, Sweden

and

ROLF WESTLUND

Division of Solid Mechanics, Chalmers University of Technology, Gothenburg, Sweden

(Received 9 December 1977; in revised form 27 June 1978)

**Abstract**—Possible sources of the observed scatter in creep deformation and rupture time are discussed. The scatter due to random material properties in creep is considered.

A constitutive equation describing these random material properties is formulated. The rupture time of a specimen under constant load is calculated using Hoff's theory of ductile rupture. Rupture is shown to occur at finite elongation, in contrast to Hoff's original analysis.

The probability distribution of the rupture time is determined with extremum value analysis and compared with experimentally observed ones.

## 1. INTRODUCTION

Creep tests are normally performed with specimens subjected to constant tensile load above half the melting temperature, on the homologous scale, of the metal. Rupture occurs after a time strongly depending on the applied stress level. At high initial stress creep rupture is normally preceded by large deformations and necking (ductile rupture). This is a stability phenomenon since the reduction of the cross-sectional area during creep causes the stress to increase. This process accelerates and finally leads to rupture. At low initial stress creep rupture normally occurs with small prior deformations (brittle rupture). This phenomenon occurs due to material deterioration caused by the stress field.

The first analysis of ductile creep rupture is due to Hoff[1]. He assumed the constitutive equation due to Norton to be valid, expressing creep strain rate in terms of true stress. Rupture was shown to take place at infinite strain. Carlson[2] showed that addition of elastic or plastic strain yields ductile instability at finite strain. Brittle creep rupture has been phenomenologically described by Kachanov[3]. He introduced a state variable, denoted damage, as a measure of material deterioration.

The observed scatter in creep deformation rate and rupture time is large for most materials. Wallis[4] gave the scatter between different test specimens a thorough statistical treatment. Observations from a number of creep tests (see Broberg[5]) show that the shape of the distribution function of the measured strain rate is independent of the stress level. Wallis has shown that the strain rate is close to log-normal distributed, i.e. the logarithm of the strain rate is normal distributed.

The observed scatter may occur due to uncontrolled variations in load, temperature, specimen geometry or material creep properties or due to unaccounted effects such as bending or friction. Hayhurst[6] has shown that the scatter can be reduced, but not eliminated, through rigorous control of the test situation. The remaining scatter must be explained as being due to inhomogeneities in the material. Chang and Grant[7] observed inhomogeneous strain along a coarse-grained aluminum specimen.

Cozzarelli and Huang[8] formulated a constitutive equation including scatter. The stresses and the deformation rate of a simple truss were determined. Huang and Valentin[9] considered creep rupture under time-varying temperature.

Broberg and Westlund[10] assumed that the scatter was due to random spatial variation of material properties in creep. The expected value and variance of the creep rate of an ordinary test specimen under steady state creep were determined. A volume effect was shown to exist, viz. The variance of the deformation rate was shown to decrease with increased specimen size.

Broberg and Westlund[11] further studied the influence of random material properties on the deformation rates of a simple hyperstatic bar system and a thick-walled cylinder under internal pressure. The scatter was assumed to be small and the stresses and strain rates were determined in statistical terms, with a perturbation method. A structural shape and size effect was shown to exist, viz. the variance of the deformation rates was shown to decrease with increased structural redundancy and material volume.

In the present paper Hoff's analysis will be retained and extended. Ductile creep rupture of specimens with random material properties will be considered. The volume effect on rupture will be analysed.

## 2. DUCTILE CREEP RUPTURE ANALYSES

### 2.1 Homogeneous creep

Hoff[1] studied the creep deformation and rupture of a specimen under constant load. He assumed the constitutive equation due to Norton to be valid. Hence

$$\frac{d\epsilon}{dt} = \dot{\epsilon}_0 (\sigma/\sigma_n)^n \quad (2.1)$$

where  $\epsilon$  denotes the creep strain and  $\sigma$  denotes the true stress. Moreover  $\dot{\epsilon}_0$  and  $n$  are temperature dependent material constants and  $\sigma_n$  is a constant introduced for dimensional purposes.

The assumption of incompressibility together with the natural strain definition yields

$$\sigma = \sigma_0 e^\epsilon \quad (2.2)$$

where  $\sigma_0$  denotes the initial stress. If the elastic strain is neglected, a differential equation for the strain follows

$$\frac{d\epsilon}{dt} = \left(\frac{\sigma_0}{\sigma_n}\right)^n \dot{\epsilon}_0 e^{n\epsilon}. \quad (2.3)$$

Ductile instability occurs, i.e. the strain and the stress tends to infinity, at time

$$t_{RH} = (\sigma_n/\sigma_0)^n / (n\dot{\epsilon}_0). \quad (2.4)$$

Thus the rupture elongation is infinite. This calculated rupture time is known to overestimate the true rupture time.

### 2.2 Inhomogeneous creep

The scatter in creep deformation and rupture time is larger than can be explained by a variation in temperature. This extra scatter may be adequately explained as an inherent material property.

When formulating a constitutive equation this scatter ought to be included. The mathematical model must, in a simple way, describe the physical phenomena. From experiments performed within a large load range (see Wallis[4]), it is observed that the scatter in strain rate is almost independent of stress level. Furthermore experiments show that Norton's law often can be used as a crude representation of the material behaviour. The scatter may be attributed to any one of the two material parameters in Norton's law (see eqn 2.1). Cozzarelli and Huang[8] proposed that all the material scatter could be represented by a variation in  $n$ . If  $n$  is assumed to vary, the scatter will vary with load level (see Broberg[5]).

In the present paper it is assumed that all the scatter can be represented by a variation in  $\dot{\epsilon}_0$ . This corresponds to a scatter that is independent of the stress level. A more sophisticated model of the material scatter ought to be coupled to a more realistic form of the constitutive equation.

As a consequence Nortons constitutive equation is reformulated as

$$\dot{\epsilon}_L = \dot{\epsilon}_0 C_L \left( \frac{\sigma}{\sigma_n} \right)^n \quad (2.5)$$

where  $C_L$  is a stochastic variable and  $L$  denotes the gauge length. If the specimens are cut from the same batch of material and tested in the same ideal creep testing machine,  $C_L$  will be dependent of the local material properties only.

It is assumed that due to the manufacturing process the material properties in creep will be inhomogeneous along the specimens. The creep strain at cross section  $x$  is written as

$$\dot{\epsilon}(x) = \dot{\epsilon}_0 C(x) \left( \frac{\sigma}{\sigma_n} \right)^n \quad (2.6)$$

where  $C(x)$  is a stationary stochastic process. This process is assumed to be continuous with such small variations that uniaxial theory is still valid. Since the specimens are cut from the same material batch,  $C$  is moreover considered to be ergodic.

The relation between global and local strain rate is

$$\dot{\epsilon}_L = \frac{1}{L} \int_0^L \dot{\epsilon}(x) dx. \quad (2.7)$$

Thus

$$C_L = \frac{1}{L} \int_0^L C(x) dx. \quad (2.8)$$

Walles[4] has shown that the strain rates are close to log-normal distributed, i.e.  $\ln \dot{\epsilon}_L$  are normal distributed, for many materials. As a consequence  $C_L$  is considered to be log-normal distributed and  $C(x)$  is assumed to be log-normal distributed.

Ductile creep rupture will occur at the cross section where the strain rate is largest. In correspondence with eqn (2.4) the rupture time follows as

$$t_R = (\sigma_n / \sigma_0)^n / (n \dot{\epsilon}_0 C_{\max}) \quad (2.9)$$

where

$$C_{\max} = \sup \{C(x) | 0 \leq x \leq L\}. \quad (2.10)$$

The rupture strain at the cross section of  $C_{\max}$  is infinite but the rupture elongation of the specimen is finite. The strongly tri-axial stress state occurring at necking is neglected (see Hoff[1]).

The rupture time due to Hoff is determined from observations of elongation rate  $\dot{\Delta} = L \dot{\epsilon}_L$  over a gauge length  $L$ . Corresponding to eqn (2.4) the calculated rupture time due to Hoff is

$$t_{RH}^C = (\sigma_0 / \sigma_n)^n / (n \dot{\epsilon}_0 C_L). \quad (2.11)$$

Thus the true rupture time

$$t_R = t_{RH}^C C_L / C_{\max} < t_{RH}^C. \quad (2.12)$$

The probability distribution of  $t_R$  may be determined from the probability distribution of  $C_{\max}$ .

Huang and Valentin[9] considered creep and creep rupture with time-varying material properties. The variation in material properties was due to temperature variations.

In the present paper creep rupture with spatial-varying material properties is considered.

3. THE DISTRIBUTION FUNCTION OF THE MAXIMUM OF THE PROCESS

3.1 *Basic assumptions*

The probability distribution of  $C_{max}$  will be determined. This maximum value of  $C$  may occur as a peak, i.e.  $dC/dx = 0$  and  $d^2C/dx^2 < 0$ . Thus  $C$  is assumed to be at least twice differentiable. The other possibility is that the maximum occurs at the boundaries of the interval. The probability distribution of  $C_{max}$  is then the joint probability distribution of the two events. Since

$$\frac{d \ln C}{dx} = \frac{1}{C} \frac{dC}{dx} \quad \{0 < C(x) < \infty | 0 \leq x \leq L\} \tag{3.1}$$

it is possible to determine the probability distribution of the normal distributed process

$$\Gamma(x) = \ln C(x) \tag{3.2}$$

instead of the arduous analysis of the log-normal distributed process  $C(x)$ .

The probability of a value of  $\Gamma_{max}$  larger than a threshold  $\xi$  is

$$P[\Gamma_{max} > \xi] = 1 - P\{[\Delta_{max} \leq \xi] \cap [\Gamma_B \leq \xi]\}. \tag{3.3}$$

Here  $\Delta$  denotes a peak and  $\Gamma_B$  denotes the value of  $\Gamma$  at the boundaries. The two events are considered independent. From eqn (3.3) then follows

$$P[\Gamma_{max} > \xi] = 1 - P[\Delta_{max} \leq \xi]P[\Gamma_B \leq \xi]. \tag{3.4}$$

These two events will now be considered.

3.2 *The probability of a peak maximum less than  $\xi$*

The distribution of peaks of  $\Gamma$  may be obtained from the joint probability density function,  $p_{\Gamma\Gamma'\Gamma''}(\gamma, \gamma', \gamma'')$ , of  $\Gamma, \Gamma'$  and  $\Gamma''$ . Here prime denotes  $d/dx$ .

The random number of peaks per unit length with a value less than  $\xi$  is (see Middleton [12]),

$$M(\xi, x) = -\Gamma''(x)u(-\Gamma'')\delta(\Gamma'')u(\xi - \Gamma). \tag{3.5}$$

Here  $u$  and  $\delta$  denotes the unit step function and the delta function respectively.

The expected value of  $M$ , if it exists, is

$$E[M(\xi, x)] = E[M(\xi)] = - \int_{-\infty}^{\infty} d\gamma'' \int_{-\infty}^{\infty} d\gamma' \int_{-\infty}^{\infty} d\gamma \cdot \gamma'' u(-\gamma'') \delta(\gamma') u(\xi - \gamma) p_{\Gamma\Gamma'\Gamma''}(\gamma, \gamma', \gamma''). \tag{3.6}$$

The properties of the  $u$  and  $\delta$  functions yield

$$E[M(\xi)] = - \int_{-\infty}^0 d\gamma'' \int_{-\infty}^{\xi} d\gamma \gamma'' p_{\Gamma\Gamma'\Gamma''}(\gamma, 0, \gamma''). \tag{3.7}$$

This equation was first obtained by Rice [13]. The expected number of peaks per unit length regardless of their magnitude is

$$E[M(\infty)] = - \int_{-\infty}^0 d\gamma'' \int_{-\infty}^{\infty} d\gamma \gamma'' p_{\Gamma\Gamma'\Gamma''}(\gamma, 0, \gamma''). \tag{3.8}$$

Rice [13] introduced the probability distribution function of the peaks, i.e. the probability that a random peak will have a value less than  $\xi$ , as

$$F_{\Delta}(\xi) = \frac{E[M(\xi)]}{E[M(\infty)]}. \tag{3.9}$$

The theoretical results of Rice is well confirmed by experiments of Huston and Skopinski[14]. Since  $\Gamma$  is normal distributed with expected value zero it follows

$$p_{\Gamma\Gamma\Gamma}(\gamma, \gamma', \gamma'') = \frac{1}{(2\pi)^{3/2}|S|^{1/2}} \exp \left[ -\frac{1}{2|S|} \sum_{j=1}^3 \sum_{k=1}^3 \bar{S}_{jk} \gamma^{(j-1)} \gamma^{(k-1)} \right]. \tag{3.10}$$

Here  $(j - 1)$  denotes the order of differentiation of  $\gamma$ . Moreover  $|S|$  and  $\bar{S}_{jk}$  are the determinant and the cofactor of the element  $(j, k)$  of the matrix of covariances

$$s = \begin{bmatrix} s_1^2 & 0 & -s_2^2 \\ 0 & s_2^2 & 0 \\ -s_2^2 & 0 & s_3^2 \end{bmatrix}. \tag{3.11}$$

Here  $s_1^2$ ,  $s_2^2$  and  $s_3^2$  are the variances of  $\Gamma$ ,  $\Gamma'$  and  $\Gamma''$  respectively. They can be calculated from the spectral density function  $\Phi_\Gamma$  as

$$s_j^2 = \int_{-\infty}^{\infty} \omega^{2j-2} \Phi_\Gamma(\omega) d\omega \quad (j = 1, 2, 3). \tag{3.12}$$

Insertion of eqns (3.10) and (3.11) and integration, first on  $\gamma''$ , yield

$$E[M(\xi)] = \frac{1}{4\pi} \frac{s_3}{s_2} \left\{ 1 + \operatorname{erf} \left[ \frac{\xi s_3}{(2s_1^2 s_3^2 - 2s_2^4)^{1/2}} \right] \right\} - \frac{1}{4\pi} \frac{s_2}{s_1} e^{-\xi^2/2s_1^2} \left\{ 1 + \operatorname{erf} \left[ \frac{\xi s_2^2}{s_1(2s_1^2 s_3^2 - 2s_2^4)^{1/2}} \right] \right\} \tag{3.13}$$

$$E[M(\infty)] = \frac{1}{2\pi} \frac{s_3}{s_2}. \tag{3.14}$$

Here erf denotes the error function.

Huston and Skopinski[14] introduced the ratio of upcrossings of the threshold zero to the total number of peaks as

$$\alpha = \frac{E[U(0)]}{E[M(\infty)]} = \frac{s_2^2}{s_1 s_3} \tag{3.15}$$

where (see Rice[13]),

$$E[U(0)] = \frac{1}{2\pi} \cdot \frac{s_2}{s_1}. \tag{3.16}$$

Insertion of eqns (3.13)–(3.15) yields

$$F_\Delta = \frac{1}{2} \{ 1 + \operatorname{erf} [(2 - 2\alpha^2)^{-1/2} s_1^{-1} \xi] \} - \frac{1}{2} \alpha e^{-\xi^2/2s_1^2} \{ 1 + \operatorname{erf} [(2\alpha^{-2} - 2)^{-1/2} s_1^{-1} \xi] \}. \tag{3.17}$$

For the limiting cases  $\alpha = 0$  and  $\alpha = 1$  the distribution function tends to normal and Rayleigh respectively.

The probability distribution function of the maximum peak is the joint probability density function of all peaks. A heuristic, and conservative, engineering approach is to consider the events of peaks as being independent. Then

$$P[\Delta_{\max} \leq \xi] = P[(\Delta \leq \xi)^{M(\infty)L}] = [F_\Delta]^{E[M(\infty)L]}. \tag{3.18}$$

This assumption is acceptable only for processes that are not of narrow-band type. Thus narrow-band processes are excluded.

### 3.3 The probability of a boundary maximum less than $\xi$

The probability distribution function, for the normal distributed process  $\Gamma$ , at one of the

boundaries is

$$F_{\Gamma_0} = P[\Gamma(0) \leq \xi] = \int_{-\infty}^{\xi} p_{\Gamma}(\gamma) d\gamma = \frac{1}{2}[1 + \operatorname{erf}(\xi/2^{1/2}s_1)]. \tag{3.19}$$

The joint probability distribution function at both boundaries is

$$F_{\Gamma_0\Gamma_L} = P\{[\Gamma(0) \leq \xi] \cap [\Gamma(L) \leq \xi]\} = \int_{-\infty}^{\xi} \int_{-\infty}^{\xi} p_{\Gamma_0\Gamma_L}(\gamma_0, \gamma_L) d\gamma_0 d\gamma_L. \tag{3.20}$$

The joint probability density function of  $\Gamma_0$  and  $\Gamma_L$  is

$$p_{\Gamma_0\Gamma_L} = \frac{1}{2\pi s_1^2(1-\rho^2)^{1/2}} \exp\left[-\frac{\gamma_0^2 - 2\rho\gamma_0\gamma_L + \gamma_L^2}{2s_1^2(1-\rho^2)}\right] \tag{3.21}$$

where the correlation coefficient is

$$\rho = \frac{R_{\Gamma}(L)}{R_{\Gamma}(0)}. \tag{3.22}$$

For ease of computation the joint distribution function is approximated as

$$F_{\Gamma_0\Gamma_L} = [F_{\Gamma_0}]^{2-\rho}. \tag{3.23}$$

This is a non-conservative approach, but it is acceptable since the errors are small. For  $\xi = 0$  the maximum error is less than 10%. The approximation is exact in the limit  $L \rightarrow 0$

$$F_{\Gamma_0\Gamma_L} \rightarrow F_{\Gamma_0} \tag{3.24}$$

and in the limit  $L \rightarrow \infty$

$$F_{\Gamma_0\Gamma_L} \rightarrow [F_{\Gamma_0}]^2. \tag{3.25}$$

3.4 *The joint probability of a maximum larger than  $\xi$*

From eqns (3.4), (3.17) and (3.23) follows finally

$$P[\Gamma_{\max} \geq \xi] = 1 - [F_{\Delta}]^{E[M(\infty)]L} [F_T]^{2-\rho}. \tag{3.26}$$

The maximum distribution function may be evaluated as soon as the autocorrelation function is known.

4. AUTOCORRELATION FUNCTIONS

Broberg and Westlund[10] assumed that the normal distributed process  $\Gamma$  was of Markov type in wide sense. Thus the autocorrelation function may be written

$$R_{\Gamma_0}(x_0) = s^2 e^{-\beta_0|x_0|} \tag{4.1}$$

where  $x_0$  is the distance between the two cross sections considered and  $\beta_0$  is a material constant.

The corresponding spectral density function is

$$\Phi_{\Gamma_0}(\omega) = \frac{1}{2\pi} \int_{-\infty}^{\infty} R_{\Gamma_0}(x_0) e^{-i\omega x_0} dx_0 = \frac{1}{\pi} s^2 \frac{\beta_0}{\beta_0^2 + \omega^2}. \tag{4.2}$$

The autocorrelation function is not differentiable, and as a consequence neither is the process. A slight modification of eqn (4.1) yields a four times differentiable autocorrelation function, and

thus a twice differentiable process,

$$R_{\Gamma_1}(x_0) = s^2(1 + 3\beta_1|x_0| + 3\beta_1^2x_0^2) e^{-3\beta_1|x_0|} \tag{4.3}$$

where  $\beta_1$  is a new material constant. The corresponding spectral density function is

$$\Phi_{\Gamma_1}(\omega) = \frac{8}{9\pi} s^2 \frac{\beta_1^5}{(\beta_1^2 + \omega^2/9)^3}. \tag{4.4}$$

The variances of  $\Gamma$ ,  $\Gamma'$  and  $\Gamma''$  follow from eqn (3.12) as

$$s_1^2 = s^2 \tag{4.5}$$

$$s_2^2 = 3s^2\beta_1^2 \tag{4.6}$$

$$s_3^2 = 81s^2\beta_1^4. \tag{4.7}$$

An infinitely differentiable autocorrelation function is

$$R_{\Gamma_2}(x_0) = s^2 e^{-(\beta_2x_0)^2} \tag{4.8}$$

where  $\beta_2$  is another material constant. The corresponding spectral density function is

$$\Phi_{\Gamma_2}(\omega) = \frac{1}{2\pi^{1/2}} s^2 \frac{1}{\beta_2} e^{-(\omega/2\beta_2)^2}. \tag{4.9}$$

The variances of  $\Gamma$ ,  $\Gamma'$  and  $\Gamma''$  again follow as

$$s_1^2 = s^2 \tag{4.10}$$

$$s_2^2 = 2s^2\beta_2^2 \tag{4.11}$$

$$s_3^2 = 12s^2\beta_2^4. \tag{4.12}$$

The three different spectral density functions are shown in Fig. 1. The material constants  $\beta_0$ ,  $\beta_1$  and  $\beta_2$  may be determined from stationary creep measurements from two series of specimens with different gauge lengths (see Broberg and Westlund[10]).

The probability distribution function of  $\Gamma_{\max}$  is evaluated for the two autocorrelation functions  $R_{\Gamma_k}$  of eqns (4.3) and (4.8) (see Fig. 2). The distribution function of  $\ln C_{\max}$  is seen to be normal distributed for small enough values of  $\beta_k L$ . When  $\beta_k L$  is increased the straight line is curved and translated.

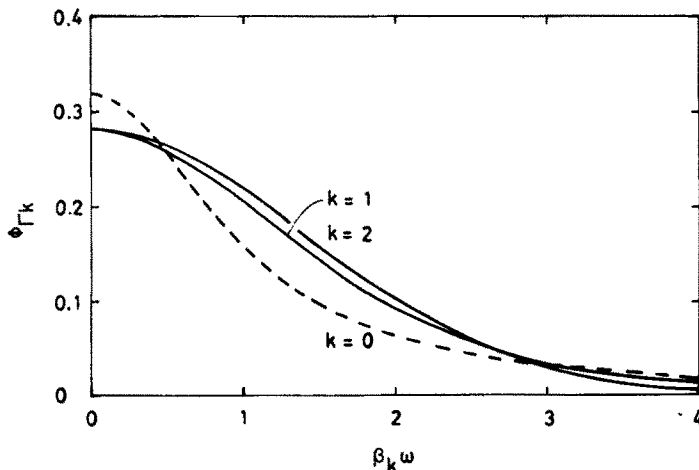


Fig. 1. Comparison of spectral density functions.

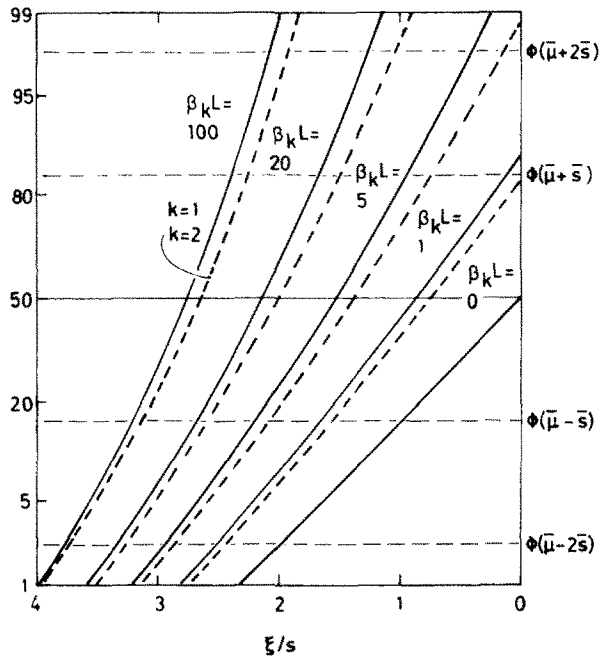


Fig. 2. Theoretical distribution function of  $\ln c_{max}$ .

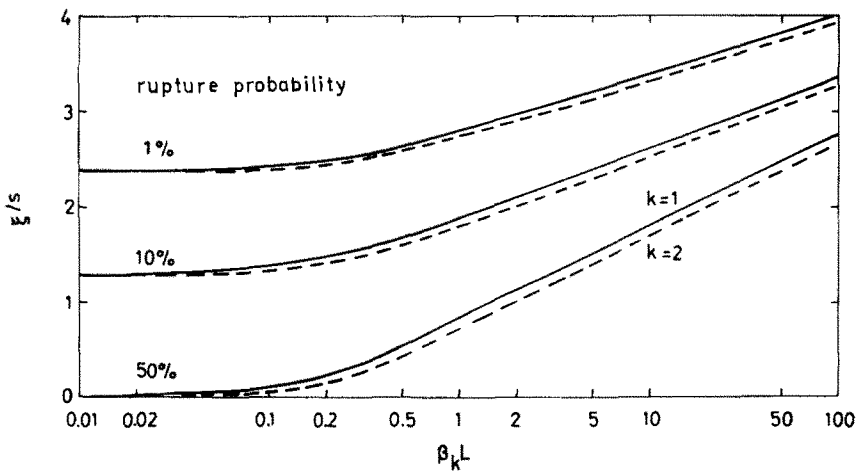


Fig. 3. Theoretical size dependence of the rupture probability.

The crossings of the thresholds 1, 10 and 50% are read and the determined rupture probabilities are redrawn in Fig. 3.

5. COMPARISON OF LOCAL AND GLOBAL SCATTER

The statistical properties, i.e. the expected value, variance and autocorrelation function, of the normal distributed process  $\Gamma = \ln C$  are

$$E[\ln C] = 0 \tag{5.1}$$

$$\text{Var}[\ln C] = s^2. \tag{5.2}$$

The two different autocorrelation functions are given in eqns (4.3) and (4.8).

The statistical properties of  $C$  are deduced as (see Broberg and Westlund[10]),

$$E[C] = e^{s^2/2} \tag{5.3}$$

$$\text{Var}[C] = e^{s^2}(e^{s^2} - 1) \tag{5.4}$$



$$R_{C1}(x_0) = \exp [s^2 + s^2(1 + 3\beta_1|x_0| + 3\beta_1^2x_0^2) e^{-3\beta_1|x_0|}] \tag{5.5}$$

$$R_{C2}(x_0) = \exp [s^2 + s^2 e^{-(\beta_2x_0)^2}]. \tag{5.6}$$

The statistical properties of  $C_L$  are deduced as

$$E[C_L] = E[C] = e^{s^2/2} \tag{5.7}$$

$$\text{Var} [C_{Lk}] = E[C_{Lk}^2] - e^{s^2} \quad (k = 1, 2) \tag{5.8}$$

where

$$E[C_{Lk}^2] = \frac{1}{L^2} \int_0^L \int_0^L E[C(x_1)C(x_2)] dx_1 dx_2 = \frac{1}{L^2} \int_0^L \int_0^L R_{Ck}(x_1 - x_2) dx_1 dx_2. \tag{5.9}$$

Since  $R_{Ck}$  depends only on the difference  $x_0 = x_1 - x_2$ , eqn (5.9) can be transformed to

$$E[C_{Lk}^2] = \frac{2}{L} \int_0^L (1 - x_0/L)R_{Ck}(x_0) dx_0. \tag{5.10}$$

Thus the global variances are

$$\text{Var} [C_{Lk}] = \frac{2}{L} \int_0^L (1 - x_0/L)R_{Ck}(x_0) dx_0 - e^{s^2} \quad (k = 1, 2). \tag{5.11}$$

A comparison with the local variance of eqn (5.4) is drawn in Fig. 4 for the two autocorrelation functions in eqns (4.2) and (4.8) for two different values of  $s$ .

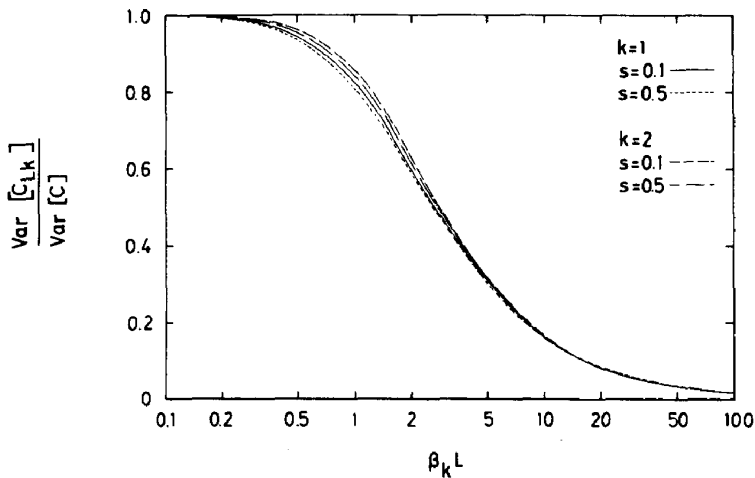


Fig. 4. Comparison of global and local scatter.

### 6. COMPARISON WITH EXPERIMENTAL OBSERVATIONS

Steady state creep rates of 23 aluminum specimens at 190°C have been measured (see Broberg and Westlund[10]). The tests were performed under rigorous laboratory conditions. The values of  $\ln C_L$  are calculated from eqn (2.5) and presented on normal distribution paper in Fig. 5. The diagram indicates normal distribution with standard deviation  $s_L = 0.42$ . The distribution of  $\ln C_L$  for 49 stainless steel specimens at 550°C is presented in Fig. 6 as a comparison. The tests were performed at the STAL-LAVAL Company[15] under commercial test conditions. This diagram also indicates normal distribution with a larger standard deviation  $s_L = 0.87$ . Both materials can be adequately described by the constitutive eqn (2.6) at the current test temperature.

It is easier to calculate the variance of  $C_L$  from the variance  $s_L^2$  of  $\ln C_L$ , obtained from a

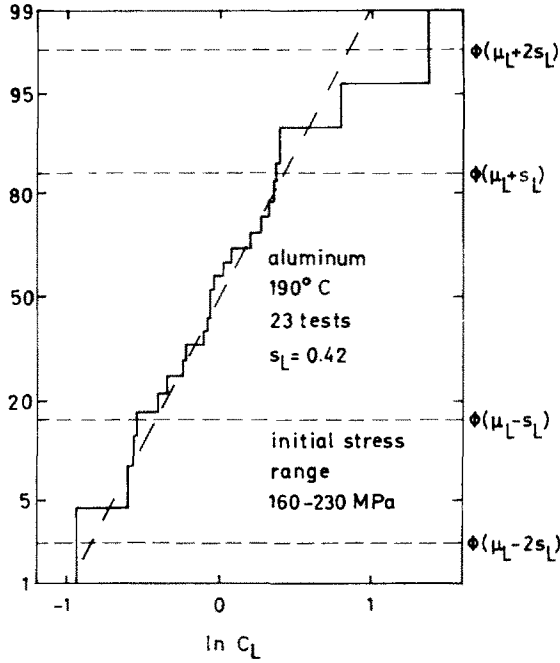


Fig. 5. Observed distribution of strain rate in aluminum.

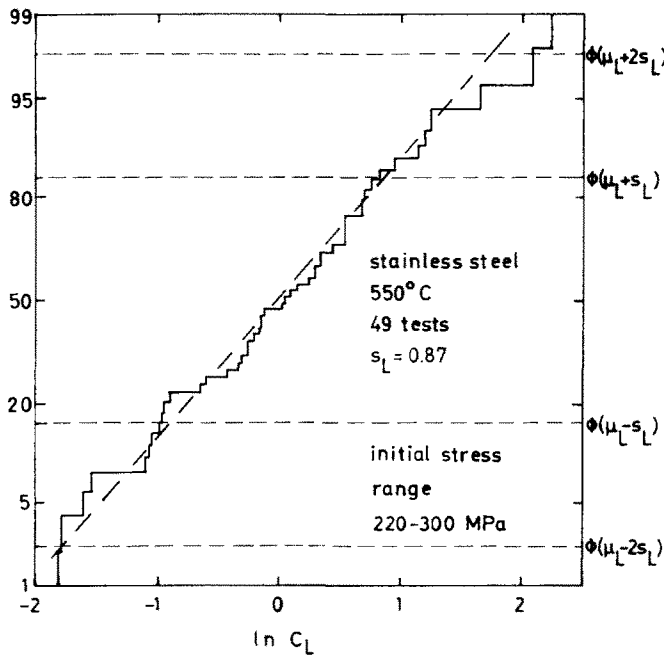


Fig. 6. Observed distribution of strain rate in a stainless steel.

normal distribution plot, than to determine it directly from the distribution of  $C_L$ . In accordance with eqns (5.2) and (5.4) follows

$$\text{Var}[C_L] = e^{s^2 L^2} (e^{s^2 L^2} - 1). \tag{6.1}$$

This variance may also be determined from eqn (5.11) for the two autocorrelation functions of eqns (4.3) and (4.8) for different values of  $\beta_k L$ . The value of  $s$ , that gives the same variance as calculated from eqn (6.1), may be iteratively determined. When  $s$  is known it is possible to redraw the theoretical distribution functions of  $\ln C_{\max}$  (see Fig. 2), vs  $\xi$  instead of vs  $\xi/s$ . The observed distribution functions of  $\ln C_{\max}$  for the aluminum and stainless steel specimens may

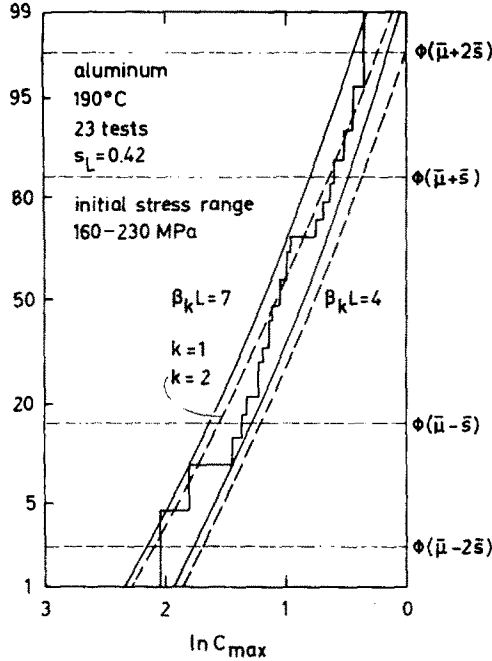


Fig. 7. Comparison of theoretical and observed rupture time distribution for aluminum.

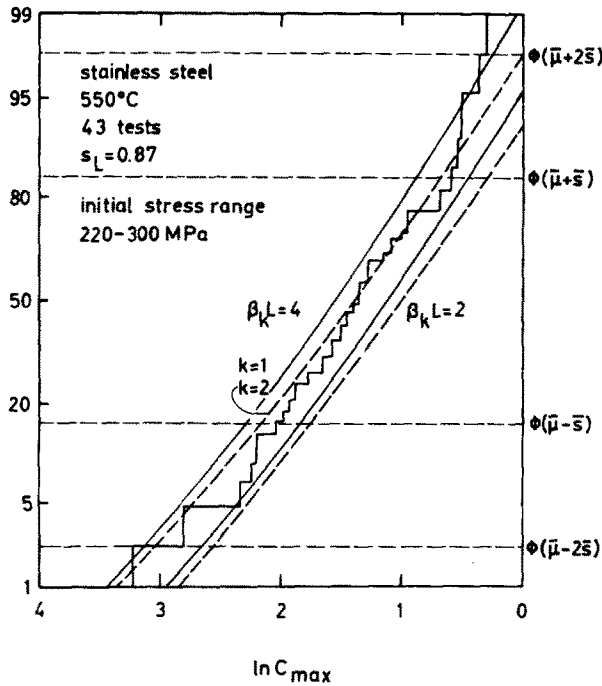


Fig. 8. Comparison of theoretical and observed rupture time distribution of a stainless steel.

be calculated from the rupture times, according to eqn (2.9). With  $\xi = \ln C_{max}$  the theoretical and experimental distribution functions of  $\ln C_{max}$  may be compared (see Figs. 7 and 8). Six of the stainless steel tests were interrupted before rupture occurred. The theoretical distributions are drawn for two values of  $\beta_k L$ , that give good agreement with the experimental distributions.

The rupture data, and the calculated Hoff rupture time, for the stainless steel specimens are shown in Fig. 9. The Hoff line coincides with the theoretical 50% rupture probability line for  $L = 0$ . The theoretical 50% rupture probability line for a length  $L > 0$  is also drawn. The distribution is seen to tend from symmetric to skew.

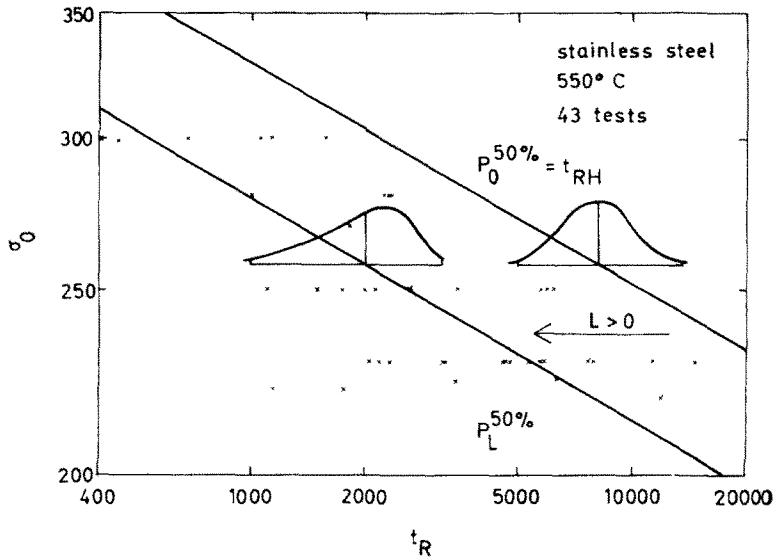


Fig.9. Logarithmic plot of stress vs rupture time for a stainless steel.

### 7. DISCUSSION

Creep rupture of specimens with random material properties has been analysed with Hoff's theory of ductile instability. The constitutive equation was formulated as a stochastic process in accordance with experimental observations. In contrast to Hoff's analysis rupture takes place at finite elongation. The distribution function of the rupture time, vs material volume, was determined with the aid of the assumption of independent peaks of the process. This distribution function was shown to be relatively independent of the choice of autocorrelation function. The distribution function of  $\ln c_{\max}$  was shown to be normal for small values of the material volume. When the material volume was increased the straight line was curved and translated. Experiments on the rupture time distributions at different specimen lengths, to confirm the theoretical analysis, have not yet been conducted. Neither have experiments been conducted where the  $\beta_k L$ , determined from steady state creep data, is compared to the  $\beta_k L$ , yielding a good agreement with rupture data. This makes it possible to determine how large part of the observed scatter that really comes from random material properties.

The analysis performed may as well be applied to determine the rupture time of structures under creep. Only ductile rupture has been considered. With the same technique it is possible to include initial, elastic or plastic, strains and also to include the brittle behaviour, due to material deterioration. The same kind of analysis should be applicable to other types of material behaviour governed by a growth law, e.g. fatigue.

### REFERENCES

1. N. J. Hoff, Necking and rupture of rods subjected to constant tensile loads. *J. Appl. Mech.* **20**, 105 (1953).
2. R. L. Carlson, Creep-induced tensile instability. *J. Mech. Engng Sci.* **7**, 228 (1965).
3. L. M. Kachanov, On the rupture times under creep. *Izv. Akad. Nauk SSSR*, No. 8 (1958) (In Russian).
4. K. F. A. Wallis, Random and systematic factors in the scatter of creep data. Aeronautical Research Council, C.P. No. 935, H.M.S.O., London (1967).
5. H. Broberg, A probabilistic interpretation of creep rupture curves. *Arch. Mech.* **25**, 871 (1973).
6. D. R. Hayhurst, The effects of test variables on scatter in high temperature tensile creep-rupture data. *Int. J. Mech. Sci.* **16**, 829 (1974).
7. H. C. Chang and N. J. Grant, Inhomogeneity in creep deformation of coarse-grained high purity aluminum. *Trans. AIME* **197**, 1175 (1953).
8. F. A. Cozzarelli and W. N. Huang, Effect of random material parameters on nonlinear steady creep solutions. *Int. J. Solids Structures* **7**, 1477 (1971).
9. W. N. Huang and R. A. Valentin, The effect of random temperature fluctuations on creep and creep rupture of cylindrical tubes. *Nuclear Engng Des.* **28**, 289 (1974).
10. H. Broberg and R. Westlund, Creep scatter as inherent material property. To be published (1979).
11. H. Broberg and R. Westlund, Creep in structures with random material properties. *Int. J. Solids Structures* **14**, 365 (1978).
12. D. Middleton, *An Introduction to Statistical Communication Theory*, p. 426. McGraw-Hill, New York (1960).
13. S. O. Rice, Mathematical analysis of random noise. *Bell System Tech. J.* **23**, 282 (1944); **24**, 46 (1945). Reprinted in N. Wax, *Selected Papers on Noise and Stochastic Processes*. Dover, New York (1954).
14. W. B. Huston and T. H. Skopinski, Probability and frequency characteristics of some flight buffet loads. *NACA TN* 3733, (August 1956).
15. Private communication, STAL-LAVAL Company, Finspång, Sweden (1972).